Monografías del Seminario Matemático García de Galdeano **33**, 377–384 (2006)

AXISYMMETRIC COMPUTATIONAL MODELLING OF A LASER INDUCED AIR PLASMA

P. Pignolet, S. Schall and S. Soubacq

Abstract. Recent developments in pulsed high voltage technologies used in some great scientific facilities (i.e. the Méajoule laser, or X radiation generator,...), have presently a large revival of interest for triggering methods. Because of numerous advantages (lowering of d.c. breakdown voltage, accuracy of shot control, variable delay without jitter, complete insulation between the triggering system and the high power electrical circuit,...), one of these consists in the use of laser triggered switches. As the relevant laser triggering is physically based on the laser induced gas breakdown process involving a plasma generation which sharply depends on complex experimental conditions (gas pressure, radiative absorption conditions,...), it is of a great importance to investigate the dynamic evolution of that phenomenon under that parametric influence. Thus, a numerical two-dimensional compressible flow simulation of the plasma expansion induced in air by a focused Nd:YAG laser beam is proposed. A modelling of the dynamic phase of laser plasma is presented. This phase, described as a strong shock wave expanding out of the focal volume, is simulated by using a two-dimensional compressible flow calculation code. The evolution of pressure, temperature, densities and velocities are analysed.

Keywords: Plasma, laser, breakdown, shockwave, 2D modelling, compressible flow

§1. The optical breakdown

When a high-energy laser beam is focused through a lens onto a gas for any given laser intensity threshold, we can observe the creation of transient plasma. The dimensions of it depend on the focal length, the divergence of the laser beam and the pressure of the gas. This breakdown mechanism is the so-called "optical breakdown" of a gas and includes a static and a dynamic part [8].

Analysis and modelling. We describe the dynamic phase of the plasma in relation to local macroscopic quantities (density, pressure, velocity and temperature). The conservation equations for mass, momentum and energy are associated with the state equation of the gas to complete the system. Moreover, a local thermodynamic equilibrium is supposed to exist and, the Saha-Eggert law allows one to evaluate the electron density. The aim of this numerical study consists in modelizing the spatio-temporal evolution of laser plasma. The radiation-gas coupling, which will macroscopically describe the behavior of the heavy particles, is done by the intermediary of a macroscopic absorption coefficient, which includes the different absorption processes (multiphoton ionization and inverse bremsstrahlung). From the initial plasma

boundary (under drastic heating induced by the laser, which is the result of high optical absorption) a rapid extension phenomenon expands through the whole space. Thus, the only worthwhile method for describing laser governed plasma expansion is the numerical solution of the hydrodynamic equations. In that case, the most important requirement is to control the discontinuity propagation in a physically consistent way. For that reason, we have used the previous method proposed by Godunov [4], which satisfies the prerequirements mentioned above.

Hypothesis. We suppose that there is a local thermodynamic equilibrium (LTE), which is the simplest hypothesis allowed for in plasma study [5, 14]. Thus, there is only a single temperature for ions, electrons and neutrals which characterize each ionized layer. The Saha-Eggert law is still valid, it allows us to determine the electron density in each layer at an equilibrium temperature T. The LTE condition is written $\Delta t > \tau_{ei}$ with Δt the integration time step and τ_{ei} the electron-ion collision time. At the beginning of the ionization process, the electrons are created in the focal volume which is a sphere of radius $r_0 = f \times l$, with f being the focal length of the lens and l the divergence of the laser beam. Thereafter, the irradiation of the plasma by the laser flux is limited to a the solid angle, even though the expansion occurs outside of this cone. We consider a two dimensional space problem. We suppose that the focal volume is uniformly lighted by the laser flux. Although we consider the plasma propagation in relation to the solid angle of the incident beam, we will consider parallel beams. Thus, the calculation of the absorbed laser energy will only be done in one direction (only *Ox*). This corresponds to the laser beam.

Equations. The dynamic state of plasma creation is described by the Euler equations for mass, momentum and energy which are in an axisymmetric form:

$$\frac{\partial \mathbf{W}}{\partial t} + \nabla.\mathbf{F}(\mathbf{W}) = 0,$$
$$\mathbf{W} = \begin{pmatrix} \rho \\ \rho u_z \\ \rho u_r \\ \rho E \end{pmatrix}, \quad \mathbf{F}_z(\mathbf{W}) = \begin{pmatrix} \rho\, u_z \\ \rho u_z^2 + P \\ \rho\, u_z\, u_r \\ (\rho E + P) u_r \end{pmatrix}, \quad \mathbf{F}_r(\mathbf{W}) = \begin{pmatrix} \rho\, u_r \\ \rho\, u_z\, u_r \\ \rho u_r^2 + P \\ (\rho E + P) u_z \end{pmatrix}. \tag{1}$$

The laser pulse has a Gaussian shape with a full width at half the maximum of $\tau_l = 12$ ns and a maximum energy of 350 mJ (Fig. 1). According to the Beer-Lambert law, radiation propagating through an absorbing medium undergoes an exponential decrease in the fluence $F(x)$ given in relation to the incident fluence F_0 such as $F(x) = F_0 \exp(-\kappa_p x)$, where κ_p is the absorption coefficient. In laser induced plasma, due to the high temperature of the plasma ($> 10^4$ K), the absorption of the laser radiation is done by inverse bremsstrahlung [9]. The absorption coefficient used, which corresponds to inverse bremsstrahlung, is the one given by Rosen *et al.* [11]:

$$\kappa_p = \left(1.37 \times 10^{-35} \frac{\lambda^3}{T^{1/2}} n_e\right)\left(n_e + \frac{n_0}{200}\right)\left(1 - \exp\left(-\frac{h\nu_l}{kT}\right)\right)$$

so κ_p in cm^{-1}, λ in micrometer, and the densities are in cm^{-3}. Considering the region of a

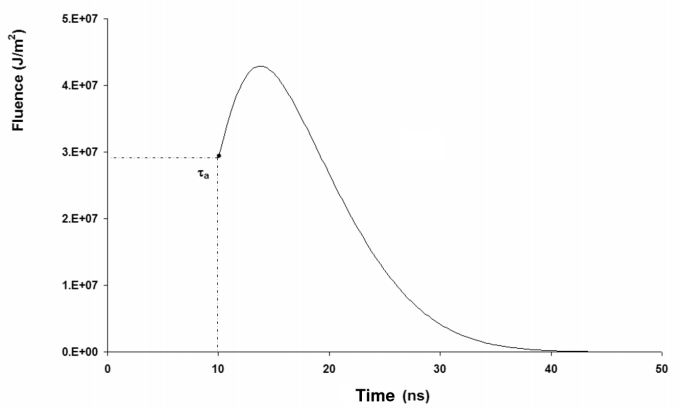

Figure 1: Experimental profile of the incident laser fluence from the time τ_a.

single ionization, the degree of ionization $\alpha = n_e/n_0$ is written as follows:

$$\frac{\alpha^2}{1-\alpha} = \frac{2}{n_0}\left(\frac{2\pi m_e kT}{h^2}\right)^{3/2} \exp\left(-\frac{U_i}{kT}\right),$$

where n_e the electron density and n_0 the neutral density at the time t.

At the time t= 0, we have reached the local thermodynamic equilibrium [15]. The value of the electron density corresponds to the final value given by the modelling of the preionization phase at the time τ_a and the equilibrium temperature is equal to T_e. Elsewhere, the gas remains cold. Thus, the initial boundaries are:

- out of the focal volume: $\rho_0 = 1$ kg/m^3, $P_0 = 10^5$ Pa, $T_0 = 350$ K, $n_e = 0$ cm^{-3};
- in the focal volume: $\rho_0 = 1$ kg/m^3, $P_0 = 10^7$ Pa, $T_0 = 4 \times 10^4$ K, $n_e = 10^{19}$ cm^{-3}.

Numerical method. The set of equations and boundary conditions previously presented are solved numerically by a two-dimensional compressible flow algorithm in a cartesian computational domain. This code (NSC2KE) solves the Euler equations which form a hyperbolic system of conservation laws. Indeed, it uses an approximated Riemann solver of Roe [10], while a spatial second order scheme is given by a MUSCL method described by Van Leer in [13]. This code has been modified in order to modelize the plasma expansion as being the electron creation due only to the laser-gas interaction. The spatial discretization of the Euler equations, based on a finite volume, can be found in [7, 2]. There is symmetry of the mesh according to the (Oy) axis. In order to distribute the laser energy in the medium, according to the Beer-Lambert law, we need to determine the origin for the abscissa x. The nodes of the mesh located on the (Ox) axis are classified in ascending order. During the calculation, from the left side of the domain, we scan these nodes and we compare the value of the corresponding electron density n_e with the initial one n_{e0}. When the inequality $n_e > n_{e0}$ is verified for a node of abscissa x_{is}, we have the position of the plasma frontier.

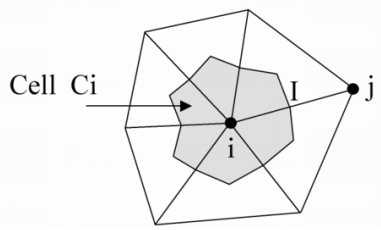

Figure 2: Cell construction around a node i.

Finite volume formulation. The variational form is obtained by multiplying (1) by a test function ψ_i and by integrating it into an open field Ω:

$$\int_\Omega \psi_i \frac{\partial \mathbf{W}}{\partial t}\,\mathrm{d}\Omega + \int_\Omega \psi_i \nabla.\mathbf{\Phi}(\mathbf{W})\,\mathrm{d}\Omega = \mathbf{0}. \tag{2}$$

We describe here the general framework of the finite volume methods to solve the system of equations. To numerically solve equation (1), we use a temporal iterative process which consists in approaching the solution at two successive moments t^n. We define the calculation time step as: $\Delta t^n = t^{n+1} - t^n$. The guiding principle of the finite volume methods consists in a division of the spatial field at each time t into finite volumes or cells defined in one dimension as follows: $C_i(t) = (x_{i-1/2}; x_{i+1/2})$.

We consider the unknown values of the function in these control volumes. More precisely, the unknown factors are supposed to represent approximations at the time t^n of the average of the unknown solution u for the cell C_i^n, that is to say:

$$u_i^n \sim \frac{1}{\Delta x_i^n} \int_{C_i} u(x,t^n)\,\mathrm{d}x.$$

Each vertex i of the mesh is associated with a cell C_i (Fig. 2) which is delimited by the medians of the close triangles of the vertex i. According to the finite volume method, we approximate the unknown factor W by a constant W_i for each cell. Moreover, we select as the test function ψ_i, which is the characteristic function associated with C_i (i.e. the function equal to 1 on the surface C_i and 0 outside the cell). The equation (2) is written as follows:

$$\int_{C_i} \frac{\partial W_i}{\partial t}\,\mathrm{d}\Omega + \int_{C_i} \nabla.\Phi(W)\,\mathrm{d}\Omega = 0 \qquad \forall i = 1,\ldots,N, \tag{3}$$

where N is the node number of the mesh. The Green formula is applied to the divergence term, thus we have:

$$\int_{C_i} \frac{\partial W_i}{\partial t}\,\mathrm{d}\Omega + \int_{\partial C_i} \Phi(W)\,\boldsymbol{\nu}\,\mathrm{d}\Gamma = 0 \qquad \forall i = 1,\ldots N, \tag{4}$$

where $\boldsymbol{\nu}$ is the normal unit external to the edge of the cell. This equation can be written as

$$\int_{C_i} \frac{\partial W_i}{\partial t}\,\mathrm{d}\Omega + \sum_{j\in v(i)} \int_{\partial C_{ij}} \Phi(W)\,\boldsymbol{\nu}\mathrm{d}\Gamma = 0 \qquad \forall i = 1,\ldots N, \tag{5}$$

where $\partial C_{ij} = \partial C_i \cap \partial C_j$ and $\nu(i)$ is the unit of nodes close to the node i. We numerically integrate this by measuring it at point I, the middle of the edge ij:

$$\int_{\partial C_{ij}} \Phi(W)\,\boldsymbol{\nu}\,\mathrm{d}\Gamma = \Phi(W_i)\boldsymbol{\eta_{ij}}, \tag{6}$$

where $\boldsymbol{\eta_{ij}} = \int_{\partial C_{ij}} \boldsymbol{\nu}\,\mathrm{d}l$. Then, we use a cell reconstruction. In the case of a first order scheme, the result of the reconstruction is a constant within the cell with the value W_I in the whole cell C_i. At the point I, the unknown factor is discontinuous (Riemann problem). Consequently, we make a decentration through discontinuity. In the case of linear conservation laws with constant coefficients, a decentration through discontinuity consists in taking $W_I = W_i$ or $W_I = W_j$ in relation to the flow direction. In the case of non-linear conservation laws, the decentration is introduced through an approximated Riemann solver. There are various decentred numerical flows and the approximated solver used here is the one proposed by Roe [10].

§2. Results and discussion

Figures 3(a), 3(b), 3(c) and 3(d) represent the profiles of the mass density, the pressure, the electronic density and the axial speed of the ionized gas for a calculation time of 50 ns, which is the total irradiation time (Fig. 1). Figures 3(e) and 3(f) illustrate the same profiles of n_e and ρ for a 2D calculation. Figure 4 shows the ratio between the axial and radial velocities for 2D and axisymetric computation. All the calculations have been made for a constant time step $\Delta t = 0.1$ ns. This time step is small enough that the energy deposition is considered to be constant during this interval. Thus, the local thermodynamic equilibrium criterion is fulfilled. More specifically, since the absorbed quantity of laser energy becomes significant, which induces the high ionization and heating of the gas, the plasma expands. The electron density reached at the end of the preionization phase is not the highest value and does not remain constant during the whole process of creation. The density sharply continues to increase due to the high absorption of the laser flux by the plasma. Meanwhile, due to expansion, the plasma goes cold in the post-discharge regime, which leads to the occurrence of recombination processes [3] and a gradual decrease in electrons [1, 12]. This fact is clearly shown by Liu [6] in the special case of a plasma created by laser ablation. Although the expansion of the plasma outside of the focal volume occurs in all directions, the visualization of the flow dynamics shows that the plasma is propagated through the privileged direction of the laser beam. The propagation velocity of the shock front (the side irradiated by the laser) is far higher than the speed of the back front. The maximum velocity reached during the laser irradiation is about 10^6 cm/s.

For the profile of density, we observe the propagation of both shock fronts, one moving towards the laser source and the other moving away from it. Each shock wave is followed by a rarefaction wave which leads to a reduction in neutral density, moving in the opposite direction.

The front temperature is propagated much more slowly than the density wave. Thus, between the position of the density front (which represents the border of the plasma) and the position of the maximum temperature; there is a colder layer which leads to the maximum absorption of radiation according to the absorption law $T^{-1/2}$.

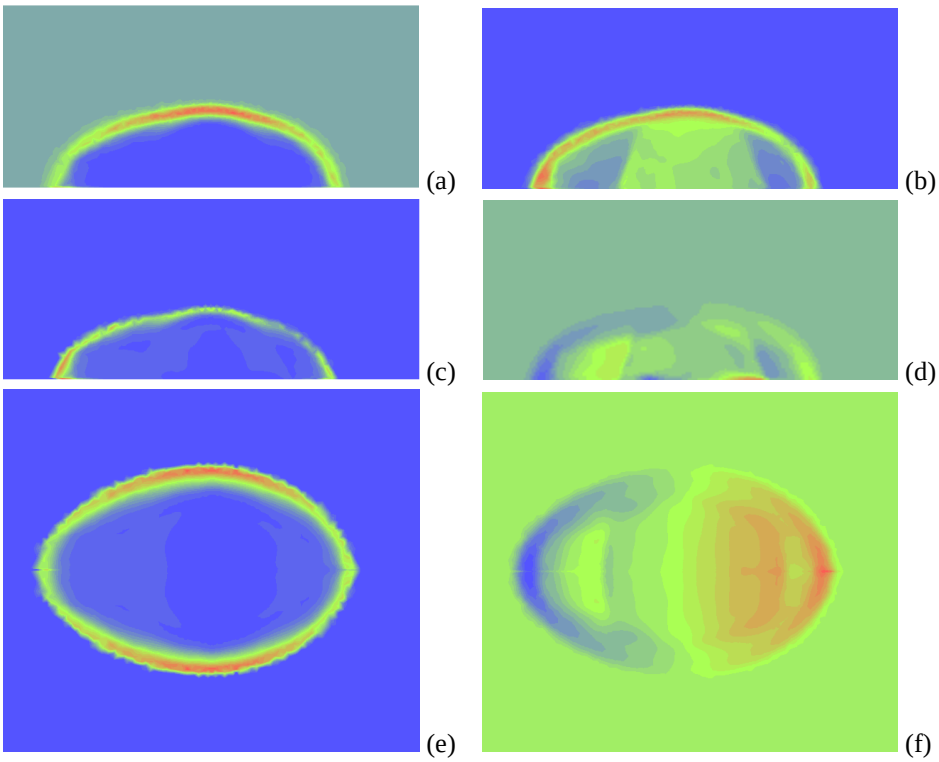

Figure 3: At $t = 50$ns. Axi computation: (a) ρ [kg/m^3], (b) P [Pa], (c) n_e [cm^{-3}], (d) u [m/s]. 2D computation: (e) n_e [kg/m^3], (f) u [m/s].

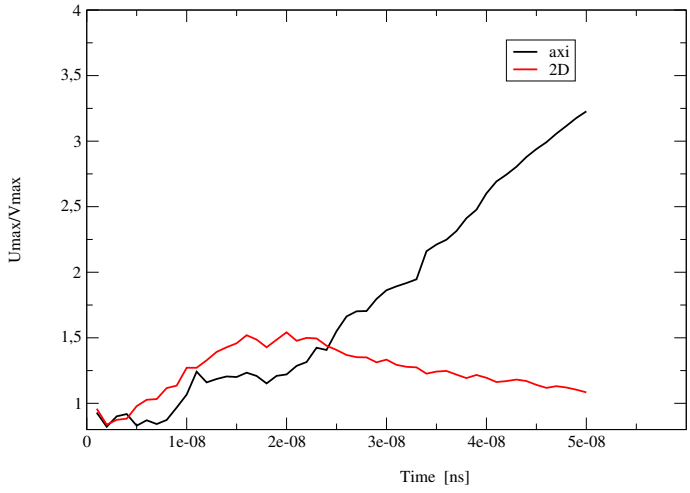

Figure 4: Ratio of axial and radial velocities for axi and 2D calculation.

Figure 3(c) represents the profile of electron density. It is noted that this profile has the same shape as the density profile. Contrary to appearances this is coherent, since the electron density is computed locally by using the Saha law and this is calculated by using the equilibrium temperature. However, this is also especially influenced by the local density ρ of the gas. The distribution of the electrons thus follows that of the atoms, because the model does not take into account electron diffusion phenomena. Furthermore, in the dynamic phase, the recombination process is not taken into account because we would need to know the distribution of the different positive and negative ions. However, this code considers only one species, the heavy particles. At the end of the laser pulse, the expansion of the plasma continues.

The variations of the different parameters remain the same as during the phase of heating and expansion, but it is noted that plasma takes a circular form in the course of time. This is in agreement with the description of the Taylor wave described by Raizer for the phase of post-discharge. We see on Figures 3(e) and 3(f) that the profiles for a 2D calculation are close to axi ones but the propagation of the shock front is quicker in the case of 2D. The geometry of the plasma is more crushed in axi than in 2D. This fact is clearly shown in Figure 4, the ration between axial and radial velocities is greater in axi calculation than in 2D after a certain delay.

§3. Conclusions

In this work, the dynamic phases of laser induced plasma have been studied. The dynamic phase of plasma creation was modelized using an aerodynamic 2D code. We treated the expansion of the plasma as being the propagation of a shock wave irradiated by a laser beam. We considered a model with a single temperature and species, that is to say the heavy particles. We supposed the system to be in local thermodynamic equilibrium and we determined the electron density by using the Saha law.

Moreover, the numerical results, given by the model for the phase of heating and expansion, describe the physical phenomena rather well. Indeed, the gas is brought up to very high temperatures ($\simeq 10^5$ K). It expands towards a privileged direction, towards the laser, and we observe the propagation of an absorption wave towards the laser source. This study was also a first attempt at describing plasma laser phenomena description by using numerical simulation for compressible flow. In future works, improvements will be added to the description of the physical model, which would take into account the Gaussian distribution of the laser energy to be closer to reality and to compare numerical results with experimental ones.

References

[1] DELCROIX, J. L. Processus atomiques et moléculaires. Gaz faiblement ionisés. Décharges dans les gaz produites par laser. *Colloque C3, Journal de Physique 29* (1968), 3–14.

[2] DERVIEUX, A. Steady Euler simulations using unstructured meshes. Von Karman Institute for Fluid Dynamics, Lecture series 1985-04, Computational Fluid Dynamics 1985. In *Partial Differential Equations of Hyperbolic Type and Applications*, Geymonat Ed. World Scientific, 1987.

[3] EL-HAMEED, A., ABOU-KOURA, G. H., AND GAMAL, Y. E. Study of recombination processes during the expansion phase of titanium-plasma produced by pico-second Nd: Glass laser radiation. *Nuclear Instruments and Methods in Physics Research B* (2003), 1–5.

[4] GODUNOV, S. K. A difference scheme for numerical computation of discontinous solutions of hydrodynamic equations. *Math. Sbornik 47* (1959), 271–290.

[5] HO, J. R., GRIGOROPOULOS, C. P., AND HUMPHREY, J. A. C. Computational study of heat transfer and gas dynamics in the pulsed laser evaporation of metals. *J. Appl. Phys. 78* (1995), 4696–4709.

[6] LIU, H., MAO, X. L., YOO, J. H., AND RUSSO, R. E. Early phase laser induced plasma diagnostics and mass removal during single-pulse laser ablation of silicon. *Spectrochimica Acta, part B, 54* (1999), 1607–1624.

[7] MOHAMMADI, B. Fluid Dynamics Computation with NSC2KE. An user guide. Rapport technique INRIA RT-0164, pp 1–70, 1994.

[8] RAIZER, YU P., AND ZEL'DOVICH, YA B. *Physics of Shock Wave and High-temperature Hydrodynamic Phenomena*, vol 1, 1966.

[9] READY, J. F. *Effects of High Power Laser Radiation*. Academic Press, New York, 1971.

[10] ROE, P. L. Approximate Riemann solvers, parameters vectors and difference schemes. *Journal of Computational Physics 4* (1981), 357–372.

[11] ROSEN, D. I., MITTELDORF, J., KOTHANDARMAN, G., PIRRI, A. N., AND PUGH, R. Coupling of pulse laser 0.35 μ m laser radiation to aluminunalloys. *J. Appl. Phys. 53* (1982), 3190–3200.

[12] TSUDA, N. AND YAMADA, J. Electron density of high-pressure argon plasma produced by XeCl excimer laser. *ECA 22c* (1998), 922–925.

[13] VAN LEER, B. Flux vector spliting for the Euler equations. *Lecture Notes in Physics 170* (1982), 405–512.

[14] VERTES, A., JUHASZ, P., DE WOLF, M., AND GIJBELS, R. Hydrodynamic modelling of laser plasma ionization processes. *International Journal of Mass Spectroscopy and Ion Processes 94* (1989), 63–85.

[15] VEYRIÉ, P. Contribution à l'étude de l'ionisation et du chauffage des gaz par le rayonnement d'un laser déclenché. Interprétation. *Le Journal de Physique 31* (1970), 41–56.

E. Schall and S. Soubacq
University of Pau, LaTEP/LMA,
1 Av. de l'Université 64000 Pau, France
eric.schall@univ-pau.fr

P. Pignolet
Laboratoire de Génie Electrique
Université de Pau et des Pays de l'Adour
Hélioparc Pau-Pyrénées
2 Avenue du Président Angot 64053 PAU
CEDEX 9 (France)
pascal.pignolet@univ-pau.fr